CROATICA CHEMICA ACTA CCACAA **73** (4) 1153–1170 (2000)

ISSN-0011-1643
CCA-2709 *Original Scientific Paper*

Substituent, Temperature and Solvent Effects on Keto-Enol Equilibrium in Symmetrical Pentane-1,3,5-triones. Nuclear Magnetic Resonance and Theoretical Studies

Predrag Novak,,# Danko Škare, Sanja Sekušak, and Dražen Vikić-Topić*

Ruđer Bošković Institute, P. O. Box 180, HR–10002 Zagreb, Croatia

Received April 11, 2000; revised May 25, 2000; accepted July 28, 2000

Keto-enol tautomeric equilibrium in several β-triketones has been investigated using NMR spectroscopy and theoretical methods. The equilibrium involves two slow and two fast enolization processes in solution. In solvents of low polarity and at room temperature, the predominant tautomeric species is the dienol form. However, the equilibrium is significantly shifted to the more polar triketo form on raising the temperature up to 140 °C and by using solvents of higher polarity. Structures and stabilities of both long- and short-lived tautomeric forms, as well as transition-state structures and barrier heights of enolization processes, were calculated using semiempirical and density functional quantum chemical methods.

Key words: pentane-1,3,5-triones, keto-enol equilibrium, nuclear magnetic resonance spectroscopy, quantum chemical calculations.

INTRODUCTION

Keto-enol tautomerism has attracted much interest during the last few decades.[1] The fact that the equilibrium involved is sufficiently slow to permit keto and enol tautomeric forms to be detected by NMR spectroscopy has

* Author to whom correspondence should be addressed. (E-mail: pnovak@rudjer.irb.hr)

\# Present address: PLIVA d.d. Research and Development, Prilaz baruna Filipovića 25, 10000 Zagreb, Croatia

allowed many investigations of these intramolecular processes. Much attention has been paid to β-diketones,[1] which are useful chelating agents for transition metal ions. Such complexes include platinum, iridium, gold and mercury.[2,3] β-Triketones, which could also be referred to as β,δ-triketones, (Scheme 1) have more possibilities to form bonds to a transition metal. However, they have been studied less frequently.[4–9] Hence, it is of practical and theoretical importance to investigate keto-enol equilibria that exist in such systems. Data so obtained would allow a better insight into the mechanism of formation, structure and properties of metal-triketone complexes, which are known to have pronounced catalytic[10] and magnetic[11] properties.

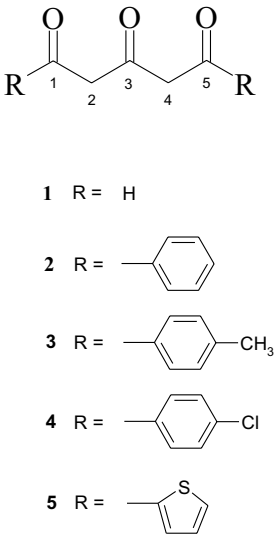

Scheme 1

Intramolecular hydrogen bonding is the main factor that governs the kinetics and influences the structure of keto-enol tautomerism in solution. Previous investigations[6] demonstrated the existence of several tautomeric forms: triketo (**A**), two monoenol ($\mathbf{B_1}$ and $\mathbf{B_2}$), and two dienol ($\mathbf{C_1}\equiv\mathbf{C_3}$ and $\mathbf{C_2}$) forms (Scheme 2). The present article deals with the effects of substituents, temperature and solvents on both the slow and fast keto-enol equilibria involving symmetrically substituted pentane-1,3,5-triones (Scheme 1). NMR spectroscopic methods and quantum chemical calculations have been combined to explore the nature of hydrogen-bonding interactions and the shift of established equilibria in different solvents and at different temperatures. The energy barriers to enolization of keto forms ($\Delta E^{\ddagger}$) have been calculated for the pentane-1,3,5-trione (model system **1**) as well.

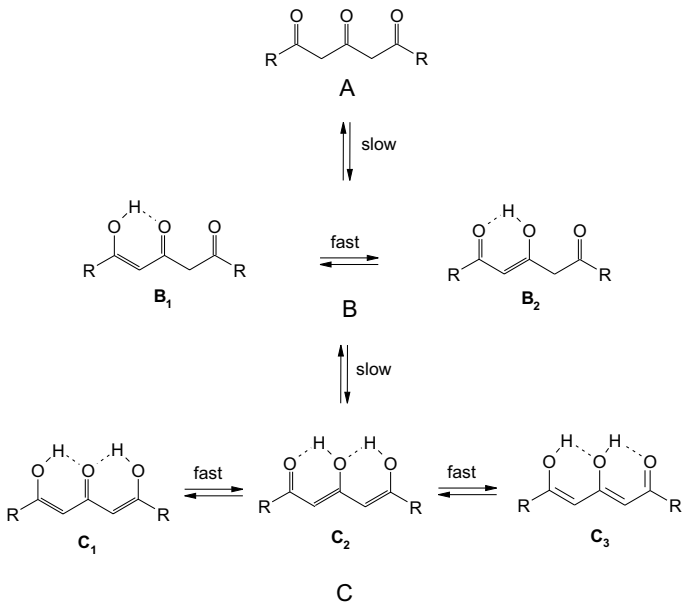

Scheme 2

Most theoretical studies of tautomeric reactions have been concerned with those occurring in the gas phase.[12] Only recently have some efforts been made to simulate tautomeric processes in solution,[13] mostly in aqueous solution.[14] Much less has been done to investigate tautomeric equilibria in non-aqueous solutions.[13,15] The self-consistent reaction field approach coupled with the *ab initio* molecular orbital theory was successfully used to describe solvent effects of relatively small molecules. Due to the size of the investigated systems here, it was not feasible to perform calculations at the *ab initio* level. Hence, semiempirical[16] and IMOMO[17] (integrated molecular orbital + molecular orbital) approaches were used to study systems **1–5** (Scheme 1). Density functional theory (DFT) was used for a detailed investigation of keto-enol equilibrium in the model system **1**. Bulk solvent effects were considered by applying the self-consistent reaction field method (SCRF)[18] to the reaction systems.

EXPERIMENTAL

Materials

1,5-Diarylpenta-1,3,5-triones, **2–5**, have been prepared by a modification of the earlier published procedure,[19] which included the treatment of the corresponding 2,6-diarylpyrones with KOH in methanol. The identity of the compounds was confirmed by IR and MS methods.[20]

NMR Measurements

^{1}H NMR spectra in $CDCl_3$, acetone-d_6, *N,N*-dimethylformamide-d_7 (DMF-d_7) and dimethyl-d_6 sulfoxide (DMSO-d_6) were recorded with a Varian Gemini 300 spectrometer operating at 7.1 T. The typical spectral conditions were as follows: spectral width 8000 Hz, acquisition time 1.9 s and 16–64 scans per spectrum. Digital resolution was 0.25 Hz per point. Deuterium from the solvent was used as the lock and TMS as the internal standard. Sample concentration was 6–10 mg mL^{-1}. Variable temperature measurements were performed in the temperature range 20–140 °C.

The content of long-lived tautomeric forms was calculated from the integrated peak intensities of the methine and methylene proton signals (Tables III and IV).

^{13}C proton decoupled and gated decoupled spectra were recorded with the same spectrometer from chloroform-d_1 solutions at 20 °C, using Waltz-16 modulation. The spectral conditions were the following: spectral width 19000 Hz, acquisition times 1–2 s and 500–2000 scans per spectrum. The concentration was 30 mg mL^{-1} and digital resolution was 0.5 Hz per point.

Complete assignment of the peaks was performed using two-dimensional homo- and heteronuclear experiments. All 2D spectra were recorded with a Varian Unity Inova 600 spectrometer operating at 14.1 T. Using gradients, DQF-COSY spectra were obtained in chloroform-d_1. 4096 points in the F2 dimension and 256 increments in the F1 dimension were used. Each experiment was measured using 1 scan, a spectral width of 5650 Hz and a relaxation delay of 1 s. The digital resolution was 2.7 and 5.5 Hz per point in the F2 and F1 dimensions, respectively. Sine-bell shifted weighting functions were applied with zero filling to 1024 points in the F1 dimension.

Using gradients, heteronuclear HSQC and HMBC spectra were obtained in chloroform-d_1 in the inverse mode (proton detection). In both types of 2D experiments, 4096 points in the F2 dimension and 256 increments in the F1 dimension were used. For each experiment, 4 scans were acquired, relaxation delay was 1 s, and spectral width was 5650 and 27580 Hz in the F2 and F1 dimensions, respectively. The digital resolution was 2.7 and 53.9 Hz per point in the F2 and F1 dimensions, respectively. For processing of the spectra, sine-bell and sine-bell shifted weighting functions were applied with zero filling to 512 points in the F1 dimension. For proton decoupling, the GARP sequence was used.

Methods of Calculations

The IMOMO method, recently proposed by Morokuma and co-workers,[17] was used to study β-triketones shown in Scheme 1. The method considers a small »model« system within a large »real« system, and applies a »higher« level calculation for the model system and a »lower« level calculation for the real system, and integrates them to define the total energy of the real system (Figure 1). The central equation of the IMOMO approach is the energy expression:

$$E(\text{IMOMO}) = E_{\text{high}} + (E_{\text{low,real}} - E_{\text{low,model}}) \quad (1)$$

As shown in Figure 1, the real system consists of set 1, set 3 and set 4 atoms and the model system **1** consists of set 1 atoms and set 2 atoms replacing set 3. »Real« systems were calculated with the PM3 hamiltonian[16] while the model system was calculated at both, PM3 and B3LYP/6–31+G(d,p) levels.[21] PM3 hamiltonian was used because of its superiority over other semiempirical hamiltonians to calculate hydrogen bonded systems.[22]

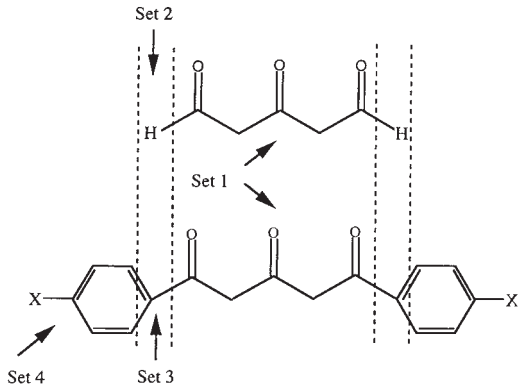

Figure 1. Definition of set1 to set4 atoms as used in the IMOMO method. Set2 atoms in the model system are replaced by set3 atoms in the real system.

The potential energy surface for tautomeric equilibria in model system **1** has been investigated within the framework of the density functional theory. Geometries were fully optimized and force constants were calculated at the B3LYP/6–31+G(d,p) level. Vibration frequencies were calculated in order to test the nature of stationary points. Diffuse functions on heavy atoms were used since it was found that they were important to predict properly the solvation effect of dipolar species.[23]

Solvent effects on molecular properties were taken into account by using the self-consistent reaction-field (SCRF)[18] method, as implemented in Gaussian94 program package[24] for *ab initio* calculations, and the COSMO[25] method as implemented in Mopac93 (Ref. 26) for semiempirical calculations. The SCRF method is based on Onsanger's reaction field theory of the electrostatic solute-solvent interaction in which the charge distribution of the solute is revealed by its dipole moment.[27] The SCRF calculations reported were carried out using the values of 4.8, 20.7, 36.7, 46.7 for the relative permittivity of $CDCl_3$, and deuterated acetone, DMF, and DMSO, respectively. The cavity radius (a_o) was calculated from the electron density, individually for each solute molecule. Geometries were fully optimized and vibration frequencies were calculated within the framework of the Onsager model. Because of the much longer computational time required, the more sophisticated isodensity polarized continuum model (IPCM)[28,29] was used only to test energetics calculated with the Onsager model.

RESULTS AND DISCUSSION

NMR Measurements

^{1}H and ^{13}C NMR chemical shifts of the relevant H and C atoms of compounds **2–5** are listed in Tables I–II, respectively. In all the studied β-triketones, proton NMR signals of the monoenol forms **B** are slightly broadened, which is due to intramolecular proton shifts (Scheme 2). In compounds **2–5**, only the signals of long-lived tautomeric forms can be observed on the NMR time scale. Therefore, one cannot differentiate between the signals of **B** and **C** forms, (Scheme 2). Instead, NMR averaged signals were detected for all **B** and **C** forms in the spectra of compounds **2–5**. This means that, for example, in the $CDCl_3$ solution of compound **2**, the two olefinic (methine) protons positioned at 6.318 ppm and 6.028 ppm (Table I) belong to the averaged monoenol forms **B** and **C**, respectively, and not to the two dienol forms **C**, as previously suggested.[8]

TABLE I

^{1}H chemical shifts (δ/ppm) of hydroxyl, methylene and methine protons in compounds **2–5**[a]

tautomer	**A**	**B**		**C**		
		δ/ppm				
group molecule	CH_2	OH	CH	CH_2	OH	CH
2	4.338	15.841	6.318	4.128	14.768	6.028
3	–	15.919	6.271	4.062	14.792	5.969
4	4.288	15.762	6.265	4.079	14.714	5.972
5	4.262	15.582	6.200	3.958	14.671	5.858

[a] Solvent = $CDCl_3$, t = 20 °C, SD = 0.005 ppm.

Chemical shifts of hydroxyl protons of forms **C** and **B** up to approximately 15 and 16 ppm, respectively, in compounds **2–5** suggest strong intramolecular hydrogen bonding. This is the main factor which stabilizes the enolic forms **B** and **C**, found to be the most abundant species (Table III).

At room temperature (20 °C), triketones **2–4** exist primarily in the dienol form **C**, while the most abundant tautomeric form for compound **5** is the monoenol form **B**. This is accounted for by the action of the polar thiophene ring, which shifts the equilibria towards the more polar triketo form **A** (Table III). In the less polar $CDCl_3$ solution, the effects of a CH_3 group and a

TABLE II

^{13}C chemical shifts (δ/ppm) of relevant carbon atoms in compounds **2–5**.[a]
(Atom numbering is depicted in Scheme 1)

		form	
molecule	C-atom	**B**	**C**
		δ/ppm	δ/ppm
2	C–1	182.135	173.764
	C–2	97.048	96.761
	C–3	191.016	194.141
	C–4	50.611	96.761
	C–5	193.928	173.764
3	C–1		173.734
	C–2		96.122
	C–3		193.878
	C–4		96.122
	C–5		173.764
4	C–1	180.928	172.687
	C–2	96.829	96.781
	C–3	190.739	193.990
	C–4	50.634	96.781
	C–5	192.571	172.687
5	C–1	180.531	168.505
	C–2	97.045	95.784
	C–3	183.914	192.890
	C–4	49.251	95.748
	C–5	186.251	168.505

[a] Solvent = $CDCl_3$, t = 20 °C, SD = 0.005 ppm.

chlorine atom attached at the *para*-position of the two phenyl rings in **3** and **4** (Scheme 1) are opposite to each other. The electron-releasing CH_3 group favours the dienol form **C** (98.7%), whereas the electron-attracting Cl atom shifts the equilibrium toward more polar tautomeric forms **B** and **A** (Table III). However, the opposite trend is observed for compounds **3** and **4** in polar DMSO solution. This implies that the electron-releasing or electron-attracting character of the substituent alone cannot account for the observed percentage of tautomeric forms in solution and that solvent effects should also be taken into account.

TABLE III

Keto-enol content and solvent effects in **2–5**[a]

		tautomer	**A**	**B**	**C**
solvent	Diel. const (*D*)	molecule		%	
$CDCl_3$	4.8				
		2	1.7	10.5	87.8
		3	0.0	1.3	98.7
		4	1.2	16.5	82.3
		5	4.1	77.9	18.0
acetone-d_6	20.7				
		2	1.8	17.5	80.7
DMF-d_7	36.7				
		2	3.5	23.6	72.9
DMSO-d_6	46.7				
		2	9.1	30.0	60.9
		3	8.7	33.4	57.9
		4	7.9	28.7	63.4
		5	37.4	50.8	11.8

[a] Temp = 20 °C, *c* = 6 mg/mL, SD = better than 0.6%.

Solvent Effects

Data from Table III clearly demonstrate that an increase in the solvent polarity increases the proportions of more polar triketo (**A**) and monoenol (**B**) forms.

Thus, in nonpolar chloroform, the content of triketo form **A** in **2** is only 1.7%, whereas it is 9.1% in polar DMSO. Consequently, the percentage of the dienol form is reduced from 88.9% in chloroform to 60.9% in DMSO. This result is in agreement with that observed for heptane-2,4,6-triones reported by Dudley *et al.*,[4] but contrary to findings for some β-diketones for which no special influence of solvent polarity was observed.[30] Although it was frequently reported that the percentage of polar keto forms in β-diketones and β-triketones depends on the solvent polarity, the shift of the equilibrium could also be related to specific interactions involving solvent molecules.

As pointed out previously, the solvents used in this investigation change the position of keto-enol equilibrium appreciably, but have only a minor influence on both ^1H and ^{13}C chemical shifts.

Temperature Effects

In order to study the effects of temperature on keto-enol tautomerism, ^{1}H NMR spectra of compounds **2**–**5** have been recorded in the temperature range 20–140 °C. The dependence of the percentage of tautomeric forms **A**, **B** and **C** on the temperature is depicted in Figure 2. It is apparent that an increase in temperature from 20 to 140 °C dramatically affects the balance at equilibrium and shifts it toward the triketo-form **A**. In all cases, the dienol form percentage rapidly decreases when raising the temperature from 20 to 140 °C. The opposite trend is observed for the content of the triketo form. Only in the case of compound **5** does the percentage of the triketo form exceed 50% at 140 °C. The content of the dienol form **C** is decreased and is as low as 3.6% in a DMSO solution of **5** (Figure 2). It is worth noting that in polar DMSO the equilibrium is already shifted toward polar **A** and **B** forms even at ambient temperature (20 °C). This experimental finding will be discussed in the following section.

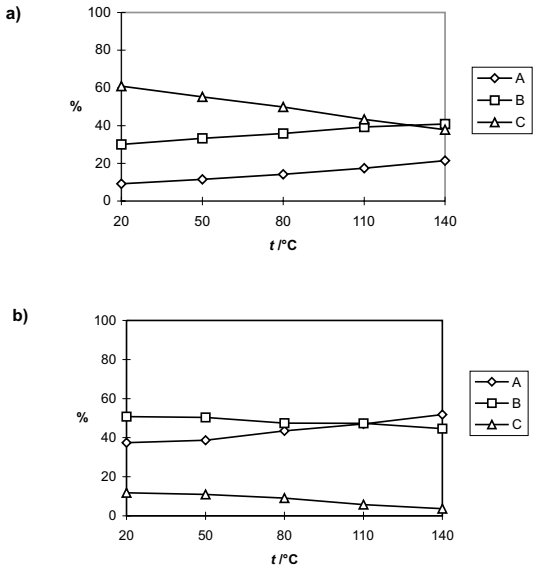

Figure 2. Temperature effects on the percentage (%) of tautomeric forms **A**, **B** and **C** in compound a) **2** and b) **5** in DMSO-d_6 solution, as determined by ^{1}H NMR.

Calculations

The geometries of the β-triketones were optimized with PM3 hamiltonian in order to investigate the stability of keto and enol forms in the gas

phase, and in four different solvents: $CDCl_3$, deuterated acetone, DMF and DMSO. It was found that semiempirical methods do not reproduce the tautomeric stability trend observed experimentally. The PM3 method predicts the tautomeric form **A** (Scheme 2) to be the most stable one. Inclusion of solvent effects does not change this trend. Due to the size of the system, density functional and *ab initio* methods were not applicable here. Therefore, the IMOMO approach was used as described in the Experimental section. Correcting the energies for the model system obtained at B3LYP/6–31+G(d,p) level changed the stability of the conformers in agreement with experimental findings.

Stability of the keto-enol forms is not affected significantly by the action of different solvents, except for compound **5**, where small solvent effects were predicted. For compound **5**, the energy difference between tautomers **B** and **C** decreases significantly from the gas phase to the polar solvent, but the calculations show that **C** is still the most stable form. This is contrary to the experimental findings, which pointed toward tautomeric form **B** as the most abundant molecular species. Modelling of the specific interactions with solvent molecules might be needed to account for this stability trend.

In all cases, enolization of the terminal carbonyl groups is preferable to that of the central carbonyl group, except again for compound **5**, for which the fast equilibrium is shifted toward $\mathbf{B_2}$ and $\mathbf{C_2}$ tautomers (Table IV). These findings were further proved with single point second-order Möller-Plesset perturbation theory[31] calculations. The largest discrepancy between the calculated and experimental results observed for compound **5** seems to be due to the deficiency of PM3 hamiltonian, used for geometry optimization, to describe hypervalent atoms like sulphur.

A small substituent effect is predicted within the IMOMO model for compounds **2**, **3** and **4**. In order to include the substituent effect at the density functional level and to test the stability of tautomeric forms for molecule **5**, energies were recalculated at the B3LYP/6–31+G(d,p) level, but results comparable with IMOMO values were obtained.

TABLE IV

Energy differences, ΔE (kJ mol^{-1}), between three tautomeric forms calculated for **2–5** at the B3LYP/6–31(d,p) level using geometries optimized at the PM3 level

molecule	**2**	**3**	**4**	**5**
ΔE_{AB}	39.3	40.6	41.4	24.3 (33.9)[a]
ΔE_{BC}	20.9	21.3	21.3	37.2 (5.4)
ΔE_{AC}	60.2	61.9	62.8	61.5 (39.3)

[a] Values in parentheses are calculated for tautomers $\mathbf{B_2}$ and $\mathbf{C_2}$ or $\mathbf{C_3}$.

To get a deeper insight into keto-enol equilibria of substituted β-triketones and to explain temperature and solvent effects on the stability of the tautomeric forms, the model system, pentane-1,3,5-trione, was investigated at the density functional level. Both slow and fast equilibria were studied taking into account the possibility of various local minima. Geometries of the most stable conformers for the five keto-enol forms of **1**, fully optimized at B3LYP/6-31+G(d,p), are shown in Figure 3.

The geometry of the tautomer form **A** is stabilized with two intramolecular hydrogen bonds between terminal carbonyl groups and hydrogen atoms from the CH_2 groups. Two different tautomers were found for both the monoenol and dienol forms. Tautomer $\mathbf{B_1}$ is planar in the gas phase but the interactions with the solvent cause bending of the terminal carbonyl group. Tautomer $\mathbf{B_2}$ is neither planar in the gas phase nor in the $CDCl_3$ and DMSO. Dihedral angles between C=O and CO(H) bonds in the gas phase and in solution are given in Figure 3. Tautomers $\mathbf{B_1}$ and $\mathbf{B_2}$ are stabilized by a strong hydrogen bond between one carbonyl group and the hydrogen atom from the enol group. The lengths of this bonds for $\mathbf{B_1}$ and $\mathbf{B_2}$ are 1.657 Å and 1.625 Å, respectively. Tautomer $\mathbf{C_1}$ has $\mathbf{C_{2v}}$ symmetry with two hydrogen

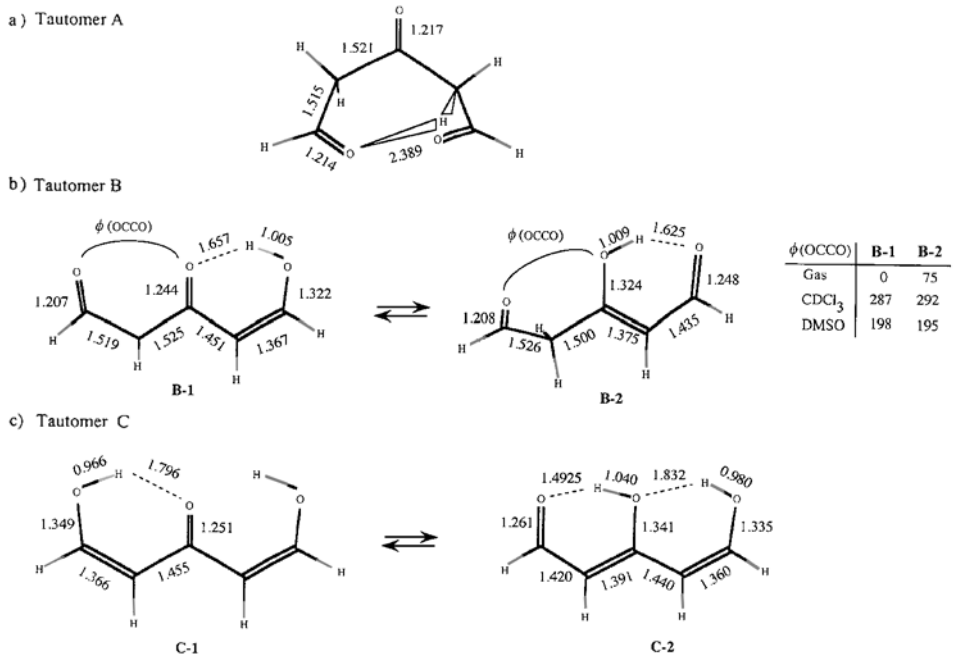

Figure 3. Selected geometrical parameters for tautomeric forms of model system **1**, calculated in the gas phase at the B3LYP/6–31+G(d,p) level of theory.

bonds of 1.796 Å. In tautomer $\mathbf{C_2}$, the symmetry is broken and two hydrogen bonds of different length are formed. The gas phase length of the shorter hydrogen bond is 1.493 Å, and that of the longer bond is 1.832 Å. When solvent effects are included, a shortening of H-bonds is observed, resulting in an increase in the tautomer stability. Due to the higher stabilization achieved through two hydrogen bonds, tautomers **C** are more stable than tautomers **B**. The length of the carbonyl C=O bond participating in hydrogen bonding changes correspondingly (Figure 3). Relative energies are defined in Figure 4 and given in Table V.

Because the gas phase results are in disagreement with experimental data (see Tables III and IV) the geometries of all tautomers were optimized including the solvent effects through the Onsanger model. Two different solvents, $CDCl_3$ and DMSO, that cover a wide range of dielectric constants were used. Only the geometry of the tautomeric form $\mathbf{B_1}$ changed significantly. The

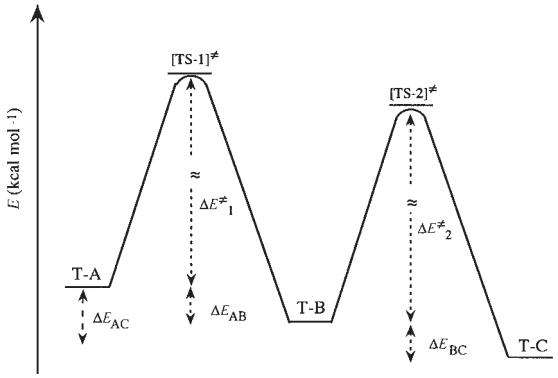

Figure 4. Energy diagram for keto-enol tautomerization of **1**.

TABLE V

Energies, ΔE (kJ mol^{-1}), of the model system **1**, optimized at the B3LYP/6–31(d,p) level in the gas phase, $CDCl_3$ and DMSO-d_6

ΔE[a]	gas-phase	$CDCl_3$	DMSO-d_6
ΔE_{AB}	–1.7	–28.5	–33.9
ΔE_{BC}	–55.6	–33.1	–35.1
ΔE_{AC}	–57.3	–61.5	–69.0
$\Delta E_1^{\ddagger}$	313.0	252.7	311.3
$\Delta E_2^{\ddagger}$	279.1	243.9	345.6

[a] Values are calculated for tautomers $\mathbf{B_1}$ and $\mathbf{C_1}$, with the terminal carbonyl group enolyzed.

most stable conformer in solution was found to be nonplanar and the dihedral angles between two carbonyl bonds, calculated in different solvents, are shown in Figure 5.

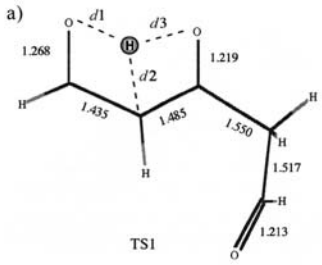

	gas	$CDCl_3$	DMSO
TS1			
*d*1	1.267	1.267	1.272
*d*2	1.519	1.529	1.512
*d*3	2.653	2.683	2.607
TS2			
*d*1	1.288	1.288	1.286
*d*2	1.504	1.511	1.507

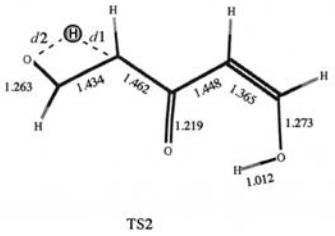

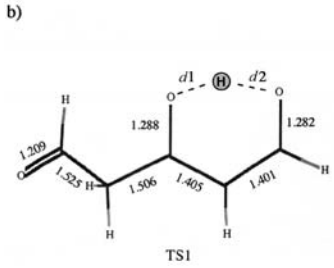

	gas	DMSO
TS1		
*d*1	1.202	1.186
*d*2	1.216	1.231
TS2		
*d*1	1.215	1.141
*d*2	1.180	1.284

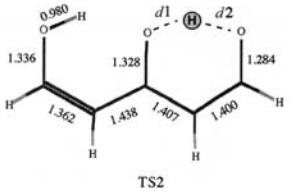

Figure 5. Selected geometrical parameters for transition-state structures determined for a) slow and b) fast keto-enol equilibria for model system **1**, calculated at the B3LYP/6–31+G(d,p) level of theory.

The described changes in geometries lead to a change in the relative stabilities in the same manner as experimentally observed by NMR. Energy differences between tautomers in fast equilibrium show that enolization of the terminal carbonyl groups is preferable to that of the central carbonyl group (Table VI).

Two transition-state structures (TS) were determined for slow and two for fast enolization processes. In the case of slow equilibria, the first transition-state structure was determined for enolization of one keto group in tautomer **A** that leads to tautomer $\mathbf{B_1}$, and the other for enolization of keto group in tautomer $\mathbf{B_1}$ that leads to tautomer $\mathbf{C_1}$. Geometries were fully optimized at the B3LYP/6–31+G(d,p) level in the gas phase, $CDCl_3$, and DMSO (Figure 5). The solvent effect on the molecular geometry is again found to be small. Both transition-state structures are reactant-like in the unimolecular rearrangement of keto to enol form, with the CH bonds being shorter than

TABLE VI

Energy differences, (kJ mol^{-1}), between tautomers in fast equilibrium for model system **1**, optimized at the B3LYP/6–31+G(d,p) level in the gasphase

ΔE	gasphase	$CDCl_3$	DMSO-d_6
$\Delta E_{B_1B_2}$	–18.8	0.0	6.3
$\Delta E_{C_1C_2}$	15.9	15.5	14.2
$\Delta E_{B_2C_2}$	–22.2	–19.7	–17.6
$\Delta E_1^{\ddagger a}$	10.0		12.6
$\Delta E_2^{\ddagger b}$	16.3		15.9

[a] Barrier height between $\mathbf{B_1}$ and $\mathbf{B_2}$ tautomers.
[b] Barrier height between tautomers $\mathbf{C_1}$ and $\mathbf{C_2}$ or $\mathbf{C_3}$.

the OH bonds. Vibrational frequencies for both transition-states were calculated and one imaginary frequency was obtained for each. Structures are characterized by a four-center H-bridge with, significantly large barrier (Figure 4, Table V). Solvent effects raise the barrier but do not change the geometry to a greater extent. The barrier to enolization of the first carbonyl group is 252.7 and 311.3 kJ mol^{-1} in the $CDCl_3$ and DMSO, respectively (Table V). The barrier to enolization of the second carbonyl group is 243.9 kJ mol^{-1} in $CDCl_3$ and 345.6 kJ mol^{-1} in DMSO. An increase in the barrier on going from $CDCl_3$ to DMSO is a consequense of the higher tautomer stabilization in a solvent of higher polarity, since species with larger dipole moments are expected to be more stabilized as the polarity of the solvent increases. Differences between barrier heights in the gas-phase and $CDCl_3$ stem from different conformations of tautomers **B**. All transition-state structures were characterized by only one negative force constant with a normal mode corresponding to the translation of hydrogen from carbon to oxygen atom.The calculated imaginary vibrational frequencies equal 1975i cm^{-1} for TS_1^{slow} and 2000i cm^{-1} for TS_2^{slow}.

Geometries of transition-state structures calculated for the fast equilibrium between $\mathbf{B_1}$ and $\mathbf{B_2}$, as well as between **C** tautomers, are shown in Figure 5. In the gas phase, the distance between the hydrogen atom and two oxygens is almost equal, while in DMSO position of the hydrogen atom it is less symmetrical. Barrier heights for the fast equilibrium are given in Table VI. The calculated barriers of only few kJ mol^{-1} are in agreement with experimental findings, which pointed to the fact that hydrogen exchange is very fast in comparison with the enolization process.

Since the barriers obtained for enolization processes are fairly high, enolization of keto forms by direct hydrogen transfer is a very slow process. Although it was already found that keto-enol tautomerizations can be catalyzed by solvent molecules,[14c] such specific interactions of **1** with solvent molecules were not found at the level of theory used here.

Finally, we want to comment on the experimentally observed temperature dependence of keto-enol equilibria. As previously pointed out, each tautomer form is stabilized by an intramolecular hydrogen bond. Increase in the temperature weakens the hydrogen bond, affecting the overall geometry. Since weaker hydrogen bonds have been formed in tautomer forms **C**, a larger temperature dependence of forms **C** than forms **B** was measured experimentally. Accordingly, weaker barriers to the rotation of the OH bond are predicted for tautomers **C**. The barrier to the rotation of the OH bond in tautomer $\mathbf{B_1}$ is 88 kJ mol^{-1} at the B3LYP/6–31+G(d,p) level. In DMSO-d_6, this barrier drops to 71 kJ mol^{-1}. The barrier to the OH rotation in tautomer $\mathbf{C_1}$ is predicted to be 63.6 kJ mol^{-1}. An increase in temperature thus results in the shifting of the equilibrium to monoenol and triketo forms. In order to quantitatively describe this behaviour, molecular dynamic simulations are needed.

CONCLUSIONS

It has been demonstrated that the keto-enol tautomerism in the β-triketones studied is strongly dependent on the temperature, solvents and substituents. NMR data have pointed toward the dienol form as the most abundant species for compounds **2**–**4**, while the monoenol form is predominant for compound **5**. The content of all tautomers, to a large extent, is affected by increasing the temperature and by changing the solvent polarity. For pentane-1,3,5-trione, the model system, calculations at the B3LYP/6–31+G(d,p) level have shown that electrostatic interactions with different solvents mostly result in small changes of the tautomer geometries, except for the case of tautomer $\mathbf{B_1}$. The dienol form was found to be the most stable in the gas phase and in $CDCl_3$ and DMSO. Enolization of the terminal carbonyl groups was preferable to that of the central carbonyl group, tautomers $\mathbf{B_1}$ and $\mathbf{C_1}$ being more stable than tautomers $\mathbf{B_2}$ and $\mathbf{C_2}$ or $\mathbf{C_3}$. Calculations at the B3LYP/6–31G+(d,p) level predicted low barriers of a few kJ mol^{-1} for the conversion from $\mathbf{B_1}$ to $\mathbf{B_2}$, and $\mathbf{C_1}$ to $\mathbf{C_2}$ or $\mathbf{C_3}$ tautomers, whereas tautomerization of tautomer **A** to tautomer $\mathbf{B_1}$ as well as to tautomer $\mathbf{C_1}$ was characterized by a high barrier of approximately 251–335 kJ mol^{-1}. The keto-enol equilibrium was shown to be only slightly affected by electrostatic solvent effects, but the change was more pronounced for barrier heights calculated

in solution. Based on the prohibitively high barriers obtained for enolization processes, enolization of keto forms by direct hydrogen transfer is expected to be a very slow process both in the gas phase and in the solvents investigated in this paper.

Acknowledgements. – This research was supported by the Ministry of Science and Technology of the Republic of Croatia (Projects No. 00980802 and 0098065). We are indebted to Dr. J. Plavec for performing some NMR measurements.

REFERENCES

1. F. Hibbert and J. Emsley, *Adv. Phys. Org. Chem.* **11** (1990) 255–379.
2. D. Gibson, J. Lewis, and C. Oldham, *J. Chem. Soc.* A (1966) 1453–1456.
3. D. Gibson, *Coordinative Chem. Rev.* **4** (1969) 225–240.
4. C. W. Dudley, T. N. Huckerby, and C. Oldham, *J. Chem. Soc.* A (1970) 2605–2607.
5. G. Grins and W. H. Watson, *Rev. Latinoamer. Quim.* **7** (1976) 31–33.
6. D. Kh. Zheglova, I. K. Kavrakova, A. I. Koltsov, and Yu. A. Ustynyuk, *J. Mol. Struct.* **195** (1989) 343–349.
7. K. B. Anderson, M. Langgard, and J. Spangent-Larsen, *J. Mol. Struct.* **475** (1999) 131–140.
8. A. G. Serrette, C. K. Lai, and M. Swager, *Chem. Mater.* **6** (1994) 2252–2268.
9. T. Sano, T. Saitoh, and J. Toda, *Heterocycles* **36** (1993) 2139–2145.
10. J. F. Wishart, C. Caccarelli, R. L. Lintvedt, J. M. Berg, D. P. Foley, T. Frey, J. E. Hahn, K. O. Hodgson, and R. Weis, *Inorg. Chem.* **22** (1983) 1667–1671.
11. P. M. Henry, X. L. Ma, G. Noronha, and K. Zaw, *Inorg. Chem. Acta* **240** (1955) 205–210.
12. J. S. Kwiatkowski, T. J. Zielinski, and R. Rein, *Adv. Quant. Chem.* **18** (1986) 85–130.
13. (a) M. M. Karelson, A. R. Katritzky, M. Szafran, and M. C. Zerner, *J. Org. Chem.* **54** (1989) 6030–6035.
    (b) M. M. Karelson, A. R. Katritzky, M. Szafran, and M. C. Zerner, *J. Chem. Soc., Perkin Trans. 2* (1990) 195–201.
    (c) A. R. Katritzky and M. M. Karelson, *J. Am. Chem. Soc.* **113** (1991) 1561–1572.
14. (a) C. J. Cramer and D. G. Truhlar, *Structure and Reactivity in Aqueous Solution* ACS Symp. Series, Washington, 1994, pp 1–9.
    (b) G.-S. Li, M. F. Ruiz-Lopez, and B. Maigret, *J. Phys. Chem.* **A101** (1997) 7885–7892.
    (c) D. Lee, C. K. Kim, B.-S. Lee, I. Lee, and B. Lee, *J. Comput. Chem.* **18** (1997) 56–69.
15. (a) M. Szafran, M. M. Karelson, A. R. Katritzky, J. Koput, and M. C. Zerner, *J. Comput. Chem.* **14** (1993) 371–378.
    (b) M. Cossi, M. Persico, and J. Tomasi, *J. Am. Chem. Soc.* **116** (1994) 5373–5378.
    (c) F. J. Luque, Y. Zhang, C. Aleman, M. Bachs, J. Gao, and M. Orozco, *J. Phys. Chem.* **100** (1996) 4269–4276.
    (d) J. Wang and R. J. Boyd, *J. Phys. Chem.* **100** (1996) 16141–16146.
    (e) P. I. Nagy and K. Takacsnovak, *J. Am. Chem. Soc.* **119** (1997) 4999–5006.
    (f) A. Broo and A. Holmen, *Chem. Phys.* **211** (1996) 147–161.
16. J. J. P. Stewart, *J. Comput. Chem.* **10** (1989), 209–220 and 221–264.

17. (a) F. Maseras and K. Morokuma, *J. Comput. Chem.* **16** (1995) 1170–1179.
(b) T. Matsubara, F. Maseras, N. Koga, and K. Morokuma, *J. Phys. Chem*. **100** (1996) 19357–19363.
(c) T. Matsubara, S. Sieber, and K. Morokuma, *Int. J. Quant. Chem.* **60** (1996) 1101–1109.
(d) S. Humbel, S. Sieber, and K. Morokuma, *J. Chem. Phys.* **105** (1996) 1959–1967.
(e) M. Svensson, S. Humbel, and K. Morokuma, *J. Chem. Phys*. **105** (1996) 3654–3661.
18. (a) C. J. Cramer and D. G. Truhlar, *Reviews in Computational Chemistry*, in: K. B. Kipkowitz and D. B. Boyd (Eds.), Vol. 6, VCH, New York, 1995, pp.1–72.
(b) J. Gao, *Reviews in Computational Chemistry,* in: K. B. Lipkowitz and D. B. Boyd, (Eds.), Vol. 7, VCH, New York, 1996, pp. 119–185.
19. K. Balenović and R. Munk, *Arh. Kem.* **18** (1946) 41–44.
20. V. Švob and D. Škare, *Rap. Commun. Mass Spectrom.* **1** (1987) 73–74.
21. (a) A. D. Becke, *J. Chem. Phys.* **98** (1993) 5648–5652.
(b) C. Lee, W. Yang, and R. G. Paar, *Phys. Rew. B* **37** (1988) 785–789.
(c) B. Miehlich, A. Savin, H. Stoll, and H. Preuss, *Chem. Phys. Lett.* **157** (1989) 200–206.
22. (a) T. J. Zelinski, D. L. Bereengard, and R. Rein, *J. Am. Chem. Soc.* **100** (1978) 6266–6267.
(b) S. Scheiner, *Theor. Chim. Acta* **57** (1980) 71–80.
(c) E. L. Cottino, K. Irving, J. Rama, A. Iglesias, M. Pauling, and D.N. Ventura, *J. Mol. Struct.* (*Theochem*) **210** (1990) 405–425.
(d) M. W. Jurema and G. C. Shields, *J. Comput. Chem.* **14** (1993) 89–104.
(e) P. Novak, D. Vikić-Topić, Z. Meić, S. Sekušak, and A. Sabljić, *J. Mol. Struct.* **356** (1995) 131–141.
(f) P. Novak, S. Sekušak, D. Vikić-Topić, and Z. Popović, *J. Chem. Soc., Faraday Trans.* **94** (1998) 1051–1056.
23. M. W. Wong, K. B. Wiberg, and M. J. Frish, *J. Am. Chem. Soc.* **114** (1992) 1645–1652.
24. M. J. Frisch, G. W. Trucks, H. B. Schlegel, P. M. W. Gill, G. B. Johnson, M. A. Robb, J. R. Cheeseman, T. A. Keith, G. A. Petersson, J. A. Montgomery, K. Raghavachari, M. A. Al-Laham, V. G. Zakrzewski, J. V. Ortiz, J. B. Foresman, J. Cioslowski, B. B. Stefanov, A. Nanayakkara, M. Challacombe, C. Y. Peng, P. Y. Ayala, W. Chen, M.W. Wong, J. L. Anders, E. S. Replogle, R. Gomperts, R. L. Martin, D. J. Fox, J. S. Binkley, D. J. Defrees, J. Baker, J. J. P. Stewart, M. Head-Gordon, C. Gonzalez, and J. A. Pople, *Gaussian 94, Revision C.2.* Gaussian, Inc., Pittsburgh PA, 1995.
25. A. Klamt and G. Schuurmann, *J. Chem. Soc., Perkin Trans 2* (1991) 531–537.
26. J. J. P. Stewart, MOPAC93, QCPE
27. L. Onsanger, *J. Am. Chem. Soc.* **58** (1936) 1486–1493.
28. (a) J. B. Foresman, T. A. Keith, M. J. Frisch, and M. Murcko, *J. Phys. Chem.* **100** (1996) 16098–16104.
(b) J. Tomasi and M. Persico, *Chem. Rev.* **94** (1994) 2027–2094.
29. K. B. Wiberg, H. Castejon, and T. A. Keith, *J. Comput. Chem.* **17** (1996) 185–190.
30. C. G. Swain, M. S. Swain, A. L. Powell, and S. Alunn, *J. Am. Chem. Soc.* **105** (1983) 502–513.
31. C. Möller and M. S. Plesset, *Phys. Rev.* **46** (1934) 618–622.

SAŽETAK

Efekti supstituenata, temperature i otapala na keto-enolnu ravnotežu nekih simetričnih pentan-1,3,5-triona. NMR i teorijska istraživanja

Predrag Novak, Danko Škare, Sanja Sekušak i Dražen Vikić-Topić

Keto-enolna tautomerna ravnoteža u nekih β-triketona istraživana je s pomoću spektroskopije NMR i teorijskih metoda. Ta ravnoteža uključuje dva spora i dva brza enolizacijska procesa u otopini. Na sobnoj temperaturi i u otapalima male polarnosti najzastupljeniji je dienolni oblik. Međutim, prilikom povećanja temperature do 140 °C te u otapalima veće polarnosti, ravnoteža se znatno pomiče prema jače polarnijem triketo obliku. Struktura i stabilnost dugo- i kratko-živućih tautomernih oblika, strukture prijelaznih stanja te barijere enolizacijskih procesa računani su semiempirijskim metodama i metodama funkcionala gustoće.